FATIGUE GROWTH BEHAVIOR OF SHORT CRACKS IN α-β-SiAlON AT 1200 °C

G.-D. ZHAN and M. J. REECE
Department of Materials, Queen Mary and Westfield College, University of London, Mile End Road, London E1 4NS, UK
J.-L. SHI and T.-S. YEN
The State Key Laboratory of High Performance Ceramics and Superfine Microstructure, Shanghai Institute of Ceramics, Shanghai 200050, P. R.. China

ABSTRACT

Experimental results are presented on subcritical crack growth under sustained and cyclic loads in gas pressure sintered (GPS) α-β-Sialon at 1200°C. Static and cyclic fatigue crack growth rates are obtained by "controlled" surface cracking from Vickers indentations in bars loaded in 4-point bending. At the lower stress intensity factors, cyclic fatigue crack growth rate is slower than that of static fatigue at the same stress intensity factor. At higher stress intensity factors, the crack growth rates both static and cyclic fatigue are almost the same. Electron microscopy analysis in the crack-tip damage zone indicates that the fatigue stresses help aid the crystallization process of the amorphous phase and lead to increase the role of dislocation plasticity during high temperature fatigue fracture.

KEYWORDS

α-β-Sialon, Fatigue crack growth, Short cracks, High temperature, Dislocation plasticity.

I. INTRODUCTION

Several reports in the literature have been concerned with the micromechanisms of elevated-temperature subcritical crack growth for structural ceramics (Ramamurty *et al.*, 1993; Ramamurty *et al.*, 1994; Han *et al.*, 1989; Liu *et al.*, 1994; Ewart and Suresh, 1992). The single-edge-notched specimens with a rather large crack have been extensively used to measure subcritical crack growth rates of high temperatures. The present investigation explored the efficacy of using multiple "controlled" surface flaws to characterize the subcritical crack growth behavior in α-β-Sialon. Controlled flaws in the form of semielliptical cracks with a range of sizes can be introduced by Vickers microhardness indentation. The important aspects of the present study were: (1)These dimensions of the controlled cracks are the same order of magnitude as those of the natural flaws and, thus, the controlled cracks simulated the subcritical crack growth behavior of natural flaws. (2)A large number of noninteracting controlled flaws were produced in a single specimen, thus offering the possibility of efficiently obtaining the statistical influence of material variability on subcritical crack growth. This first report will focus on the results obtained at 1200°C which revealed some novel crack-tip phenomena.

II. EXPERIMENTAL PROCEDURE

2.1 Material and Specimens Preparation

The starting powders used in this study were Si_3N_4, AlN, Al_3O_2 and Y_2O_3. The mixtures of powders were milled in ethanol for 24 h in an alumina jar, using sintered silicon nitride grinding media. After the powder mixtures were dried, they were die-pressed into bars under 20 MPa and then isostically pressed under a pressure of 250 MPa. Pressed compacts were placed in covered graphite crucible with a protective powder bed of 90wt% Si_3N_4 + 10wt%BN, and then sintered at 1950°C under 1.5 atm nitrogen pressure for 2 h in a gas pressure sintering furnace. Flexural strength was measured in 4-point bending at room temperature (650MPa) and fracture toughness measurements were performed on the polished surfaces of the fatigue specimens using indentation techniques (8.5MPam$^{1/2}$). The X-ray diffraction analysis of the sample indicated the phase compositions of the sample after GPS contain α-Sialon (30vol%) and β-Sialon (70vol%) as the two major crystalline phases with some grain boundary phases.

Specimens were rectangular bend bars with dimensions of 40 mm x 8 mm x 3 mm. The tensile surface of these specimens was finely ground along the long axis, and then polished using a 1 μm diamond paste to obtain a good finish. A series of Vickers indents was introduced on the tensile surface at different indentation loads. These indents were 1.5 mm apart and carefully aligned so that the corner cracks emanating from the indents were all parallel or perpendicular to the long axis of the specimen. 4-point bending configuration with a inner span of 10 mm and an outer span of 30 mm was used. Regardless of the contact conditions at these loading points, the linear stress distribution can be accurately determined. This configuration provided data acquisition over a relatively broad range of crack growth from one specimen. For each crack, the initial surface crack length and final length can be recorded. Because these indentation cracks were of various initial lengths, they grew to various lengths during fatigue testing. Thus, there were sufficient crack length data from each test to calculate crack growth rates and stress intensity factors.

2.2 Fatigue tests

Cyclic bending fatigue tests were conducted using commercial servodraulic machine Instrong 8501 operated under load control, with a sinusoidal wave form at a frequency of 10Hz and load ratios R (minimum/maximum loads) of 0.1. The specimen was first heated to 1200°C at a rate of 30 °C/min, and then slowly loaded until the desired stress level was reached. After a certain time period (predetermined as 1/5 or 1/10 of the failure time), the load was removed and the furnace was cooled down. The oxide layer on the specimen surface was mildly polished (in the case of the in-air test), and then the surface crack length was measured by a traveling microscope at a magnification of 200x. When the specimen did not fail, a room temperature fracture test was conducted. For comparison, static fatigue tests at the same temperature and maximum stress were also conducted. Following completion of these tests, the fracture surfaces were examined with scanning electron microscope(SEM) in order to measure the size and shape of the initial and the critical cracks. In addition, thin sections were sliced out of the fatigue samples for TEM and HRTEM analysis. In order to ensure that the damage observed in the crack-tip region was caused by high temperature mechanical loads and not by the TEM specimen preparation techniques, TEM foils were also prepared from the as-received (untested) material, using the same foil preparation techniques, and examined for comparison purposes.

2.3 Data processing

The applied stress intensity factor at the crack tip subject to pure bending was calculated from the finite element analysis of Newman and Raju (1979) for three-dimension semiellipitical surface cracks in terms of crack depth, a, half crack length, c, specimen thickness and width, b and t, geometric factors, ϕ and Q, and remote (outer surface) bending stress, σa:

$$K_{app} = H\sigma a\,(\pi a/Q)^{1/2}\,F(c/a,\ c/b,\ c/t,\ c/b,\ \phi) \qquad (1)$$

where H is the bending multiplier and F is a geometric function. The aspect ration, c/a, for the semiellipitical crack was approximated by using an empirical equation recommended by ASTM E740 (1983):

$$a/c = a/b + 1 \qquad (2)$$

The residual stress intensity factor, Kr, from the residual crack-opening stress was calculated (Marshall and Lawn, 1980) in terms of indentation load, P, and the half crack length, c, by:

$$K_r = \chi\, P\, c^{-3/2} \qquad (3)$$

where the prefactor χ is a material constant, depending on elastic modulus and microhardness. Thus, total stress intensity factor at crack-tip, K_I, for the median crack is given by the summation of Eqns. (1) and (3), i.e.:

$$K_I = K_{app} + K_r \qquad (4)$$

Under such a driving force, assume that a time-based fatigue crack growth rate, da/dt, is a function of the stress intensity factor and can be expressed by the equation:

$$da/dt = A\,(K_I)^n \qquad (5)$$

where A and n are constants, which can be obtained by least-squares fitting of the measured crack growth data, and K_I is the stress intensity factor at the crack tip. The conventional average method was performed, i.e., the average crack growth rate for each indent was obtained by dividing the total crack extension by test duration, and the average stress intensity factor was the mean value of these stress intensity factors associated with the initial and final crack lengths. For static fatigue, K_I is constant until crack extension. For cyclic fatigue, K_I varies from a minimum (K_{min}) to a maximum (K_{max}) during per cycle. For the latter case, K_I was replaced by K_{max} or ΔK in the present study.

III. RESULTS AND DISCUSSION

3.1 High-Temperature Crack Growth Behavior

Figure 1 shows the relationship between fatigue crack growth velocity, da/dt, and maximum stress intensity factor Kmax, for α-β-Sialon ceramic composite subjected to cyclic tension

loading at 1200 ^{0}C and cyclic frequency of ν=10Hz and load ratio of 0.1. Note that, the cyclic fatigue crack growth per unit time is defined as

$$da/dt = da/dN \times \nu \qquad (6)$$

and the maximum stress intensity factor is given

$$K_{max} = \Delta K/(1-R) \qquad (7)$$

The static fatigue crack growth velocity, da/dt, is also plotted in Fig.1 against the sustained stress intensity factor, K_I. It is interesting to note that several features in Fig.1 which are compared crack growth rates at the same K_{max} under both cyclic and static fatigue loading are apparent. First, the cyclic fatigue crack growth per unit time (characterized in terms of K_{max}) is similar to that of static fatigue which has three characteristic regions with an almost flat plateau region. Second, the crack growth retardation due to cyclic fatigue loading is much more pronounced at lower stress intensities, however, the crack growth behavior under both cyclic and static loading is almost the same at higher stress intensities. Third, the cyclic fatigue crack growth threshold is lower than that of static one. These observations indicate that the crack growth mechanism of high temperature cyclic fatigue at lower stress intensity are different from that of static fatigue and therefore it isn't only time-dependent.

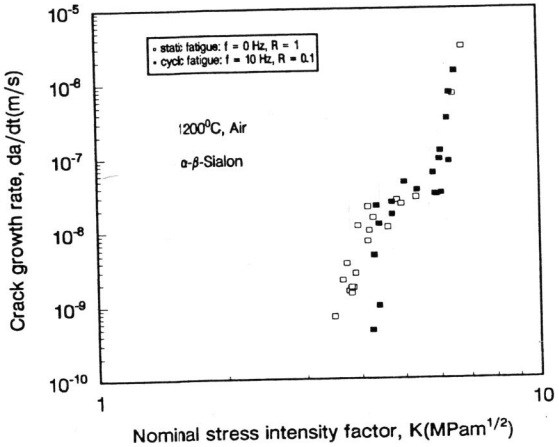

Fig.1 Variation of crack growth velocity, da/dt, as a function of applied stress intensity factor, K, for static crack growth in α-β-Sialon ceramic composite at 1200 °C air. Also shown are cyclic fatigue crack growth velocities, da/dt = (da/dN)x f, as a function of the maximum stress intensity factor, $K_{max} = \Delta K/(1-R)$, for frequencies ν = 10 Hz and load ratio, R = 0.1

The above static and low cycle fatigue crack growth behavior of α-β-Sialon with the large elongated β-Sialon grains at 1200 ^{0}C in air revealed that slow crack growth was inhibited under cyclic versus static loading in lower stress intensity factor region. The slower crack growth rate arising from the unloading portion of the cycle may be due to the following reasons: Pullouts of elongated grains were enhanced during cyclic loading. At high temperatures and lower stress

intensities, traction of grain boundary sliding is sufficiently reduced to allow much more grain pullouts without grain fracture. In α-β-Sialon made of equiaxed α-Sialon grains and whisker-like β-Sialon , bridging of crack faces by many pullouts of whisker-like β-Sialon grains in the wake of crack tip can shield the crack tip from the applied stress intensity and the effective stress intensity at crack tip was somewhat reduced. However, at higher stress intensity factor, the chance of breaking grains at the crack tip before their pullout is substantially increased, and leads to reduce the above shielding mechanism of crack tip. Therefore, the crack growth rates at lower stress intensity factor are slower under cyclic loading than under static loading, and they are almost the same at higher stress intensity factor. This is in agreement with the results of Liu *et al.*, (1994).

3.2 Crack growth mechanisms at 1200 ^{0}C

Figure 2 is transmission electron micrographs of the fatigue crack-tip regions in the ceramic material subjected to a sustained K of 5.5 MPam$^{1/2}$ in 1200^{0}C. Extensive cavities at multiple grain junctions can be clearly seen from Fig.2. Cavity growth along an interface is also clearly evident from Fig.2. However, TEM observations of the specimens subjected to cyclic fatigue crack growth experiments at 1200 ^{0}C showed that the extent of such cavitation was to low to quantify. However, TEM observations of the specimens subjected to cyclic crack growth tests at ΔK = 6.0 MPam$^{1/2}$ in 1200°C showed that the presence of dislocations within the matrix grains ahead of the fatigue crack tip can be noted (Fig.3(a)). High resolution transmission electron microscopic observations of crack-tip damage (Fig.3(b)) further reinforced the TEM observations. It cannot be conclusively shown from our present microscopy work whether these dislocations are due to cyclic loading at high temperatures or it occurs during processing of this material. However, such dislocations have not been observed in the as-received untested material in the present study. Also, the TEM examination revealed that the glassy phase at the grain boundaries in as-received GPS Sialon had crystallised during high temperature cyclic fatigue tests, as shown in Fig.4. It seems that in addition to temperature, the applied fatigue stresses will help aid the crystallization process of the amorphous phase.

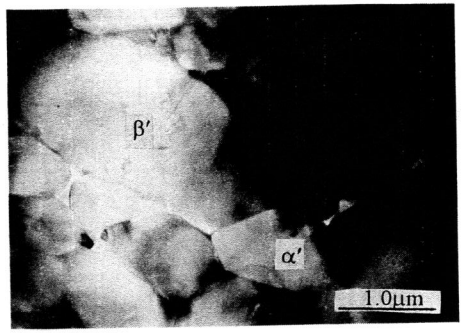

Figure 2 Transmission electron micrographs of the fatigue crack-tip regions in the ceramic material subjected to a sustained K of 5.5 MPam$^{1/2}$ in α-β-Sialon ceramic composite at 1200°C air showing extensive cavities at multiple grain junctions and cavity growth along an interface

(a)

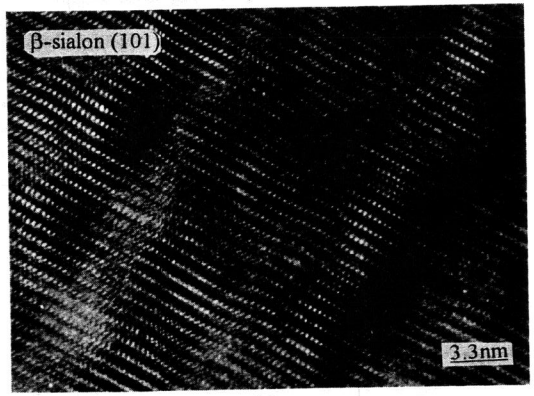

(b)

Figure 3 (a) Transmission electron micrograph micrograph of the specimens subjected to cyclic crack growth tests at $\Delta K = 6.0\ MPam^{1/2}$ in 1200°C showing the presence of dislocations within the matrix grains ahead of the fatigue crack tip. (b)High resolution transmission electron microscopy (HRTEM) micrograph showing dislocations within the β-SiAlON [101] grain

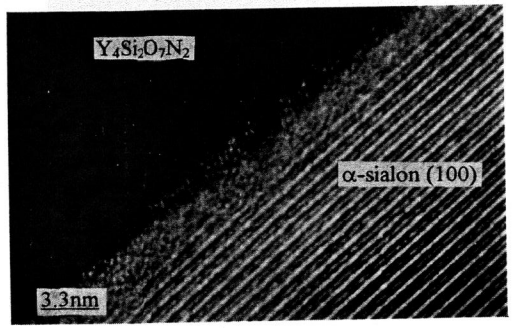

Figure 4 High resolution transmission electron microscopy micrograph of a cyclic fatigue tested sample of the α-β-Sialon material showing crystallization of amorphous phases at a triple grain junction

One of the necessary conditions for stable crack growth is that nonlinear deformation and damage processes exists at the crack-tip region (Lin *et al.*, 1993). In metals and alloys, fatigue damage is attributed to irreversible plastic deformation caused by dislocation motion. This process is not considered to be the dominant one for room temperature fatigue of ceramics. However, it might be plausible for the fatigue of some ceramics at high temperatures where the dislocation motion is active (Ramamurty *et al.*, 1993). Our studies in the vicinity of crack tips had showed dislocations within the β-Sialon grains in specimens subjected to cyclic loads at 1200 °C. This dislocation activity may be one of the mechanisms of subcritical crack growth and thus its contribution for nonlinear deformation may not be neglected under cyclic loading. The results of many studies (Ramamurty *et al.*, 1993; Ramamurty *et al.*, 1994) showed that preexisting and/or in situ-formed glass phases play a strong role in influencing the high temperature crack growth in silicide-based material. The main effects of glass phase on crack growth can be summarized as follows:(1)Enhanced propensity for interfacial cavitation, microcracking, and diffusional processes; and (2)Suppression of possible dislocation plasticity within the matrix, by the easier separation of grain boundaries and interfaces. Our experimental serults showed that the applied cyclic fatigue stresses helped aid the crystallization process of the amorphous phase. This led to decrease the content of glassy phase and the width of interfacial phase, so that grain boundary slide became difficult. Consequently, under large applied stress, it would lead to local deformation and increase the role of dislocation plasticity during high temperature fatigue fracture.

IV. CONCLUSION

Based on a study of static and cyclic fatigue crack growth behavior from Vickers indentation in α-β-Sialon at 1200 °C air, the following conclusions can be drawn:

(1)An effective test method by multiple controlled Vickers flaws in four-point bending configuration was developed for measuring the whole stages of crack growth rate in fatigue testing of structural ceramics at high temperatures.
(2)At lower stress intensities, cyclic fatigue crack growth rate was slower than that of static fatigue with the same stress intensity factor. At higher stress intensities, the crack growth rates both static and cyclic fatigue were almost the same.
(3)In addition to high temperature, the fatigue stresses help aid the crystallization process of the amorphous phase and lead to increase the role of dislocation plasticity during high temperature fatigue fracture.

REFERENCES

Ramamurty, U. , Kim, A. S., Suresh, S. and Petrovic, J. J. (1993). Micromechanisms of creep-fatigue crack growth in silicon-matrix composite with SiC particles, *J. Am. Ceram. Soc.*, **76**, 1953-64

Ramamurty, U., Suresh, S. and Petrovic, J. J. (1994). Effect of carbon addition on elevated temperature crack growth resistance in (Mo, W)Si_2-SiCp composite, *J. Am. Ceram. Soc.*, **77**, 2681-88

Cinibulk, M. K. and Thomas, G. (1990). Grain-boundary phase crystallization and strength of silicon nitride sintered with a YSiAlON glass, *J. Am. Ceram. Soc.*, **73**, 1606-12

Han, L. X. and Suresh, S. (1989). High-temperature failure of an alumina-silicon carbide composite under cyclic loads: mechanisms of fatigue-crack tip damage, *J. Am. Ceram. Soc.*, **72**, 1233-38

Liu, S. Y. , Chen, I.-Y and Tien, T.Y(1994). Fatigue crack growth of silicon nitride at 1400 ^{0}C: a novel fatigue-induced crack-tip bridging phenomenon, *J. Am. Ceram. Soc.*, **77,** 137-42

Ewart, L. and Suresh, S.(1992). Elevated temperature crack growth in polycrystalline aluminia under static and cyclic loads, *J. Mater. Sci.*, **27,** 5181-91

Marshall, D. B. and Lawn, B. R. (1980). Flaw characteristic in dynamic fatigue: the influence of residual contact stresses, *J. Am. Ceram. Soc.*, **63,** 532-36

Newman, J. C. Jr., and Raju, I. S.(1979). Analyses of surface crack in finite plate under tension or bending loads," NASA Technical Paper 1578 (available from National Technical Information Service, Springfield, VA)

ASTM Standard E.740-80, Standard recommended practice for fracture testing with surface-crack tension specimens, in ASTM Annual Book of Standard, vol.3.01, pp740-50. American Society of Testing and Materials, Philadelphia, PA, 1983

Lin, C.-K. Jack, Jenkins, M. G. and Ferber, M. K. (1993). Tensile dynamic and static fatigue relations for a HIPed silicon nitride at elevated temperatures, J. Europ. Ceram. Soc., **12**, 3-13